

Structure/Function Studies and the Effects of Memantine in Monkeys with Experimental Glaucoma

B'Ann T. Gabelt,¹ Carol A. Rasmussen,¹ Ozan Y. Tektas,² Charlene B. Y. Kim,¹ John C. Peterson,¹ T. Michael Nork,¹ James N. Ver Hoeve,¹ Elke Lütjen-Drecoll,² and Paul L. Kaufman¹

PURPOSE. The scanning laser polarimetry with variable corneal compensation (GDx VCC) methodology was established and verified in monkeys with experimental glaucoma (ExpG). Terminal GDx parameters were correlated with axon counts and electrophysiologic measures. The effects of memantine on these parameters were investigated.

METHODS. ExpG was induced in monkeys and intraocular pressure monitored weekly. Some monkeys received memantine in their diet before and after ExpG induction (1-10 months). GDx VCC scans, stereophotographs, and multifocal visual evoked potential (mfVEP) data were collected at baseline and every 6 to 8 weeks until euthanasia. Optic nerves were prepared for axon counting and other morphologic analysis.

RESULTS. There was no difference in IOP elevation exposure between memantine-treated and no-memantine-treated monkeys. The percentage of the optic nerve area composed of connective tissue septa was significantly greater in ExpG eyes than in Fellow eyes. There was a strong positive correlation between axon counts and terminal GDx parameter measures. Animals not receiving memantine exhibited significantly lower mfVEP amplitudes in ExpG eyes compared with the ipsilateral baseline or the final value in the Fellow eye. ExpG eyes from memantine-treated animals had higher overall mean amplitudes that were not significantly different relative to the ipsilateral baseline and final amplitudes in the Fellow eye.

CONCLUSIONS. The authors' studies confirm that GDx VCC can be utilized in monkey ExpG studies to detect early retinal structural changes and that these changes are highly correlated with optic nerve axon counts. These structural changes may or may not lead to central functional changes as shown by the mfVEP in response to investigational therapies. (*Invest Ophthalmol Vis Sci.* 2012;53:2368-2376) DOI:10.1167/iops.11-8475

From the ¹Department of Ophthalmology and Visual Sciences, University of Wisconsin-Madison, Madison, Wisconsin; and the ²Anatomy Institute LS II, University of Erlangen-Nürnberg, Erlangen, Germany.

Supported by grants from NIH/NEI (R01 EY002698), (R01 EY014041), (P30 EY016665); Research to Prevent Blindness, Inc., New York, NY; unrestricted departmental and Physician-Scientist awards; Ocular Physiology Research and Education Foundation; and the Walter Helmerich Chair from the Retina Research Foundation.

Submitted for publication August 25, 2011; revised January 17, 2012; accepted February 29, 2012.

Disclosure: **B.T. Gabelt**, None; **C.A. Rasmussen**, None; **O.Y. Tektas**, None; **C.B.Y. Kim**, None; **J.C. Peterson**, None; **T.M. Nork**, None; **J.N. Ver Hoeve**, None; **E. Lütjen-Drecoll**, None; **P.L. Kaufman**, None

Corresponding author: Paul L. Kaufman, University of Wisconsin-Madison, Ophthalmology and Visual Sciences, 2828 Marshall Court, Suite 200, Madison, WI 53705; plkaufma@mhub.ophth.wisc.edu.

Glaucoma is an optic neuropathy characterized by the pathological loss of retinal ganglion cells (RGCs) and their axons.¹ The experimental glaucoma (ExpG) model in nonhuman primates² is useful for evaluating potential therapies for human glaucomatous optic neuropathy.³ It is the most objective model for evaluating the correlation of various diagnostic measures for glaucoma since the glaucoma eye can be compared with the control eye of a single subject. Ocular tissue can be collected immediately after death at various stages of damage.⁴

In glaucoma, the loss of RGCs can be detected structurally as a thinning of the retinal nerve fiber layer (RNFL) and neuroretinal rim.⁵ Several imaging technologies have been developed to evaluate the optic disk and RNFL.⁶ Scanning laser polarimetry with variable corneal compensation (GDx VCC) is one technology that has been used successfully in humans to follow progressive RNFL loss in glaucoma patients that show progression in optic disc stereophotographs or mild to moderate visual field defects.^{7,8}

Adaptation of imaging technologies for use with nonhuman primates can be challenging because of their inability to fixate on a target if anesthesia is used. Alternatively, monkeys may be trained to fixate on a target after considerable investment in time. However, the numbers of other parameters to be measured and the required experimental manipulations may not be practical with a conscious model.

We describe here a technique for obtaining reproducible scanning laser polarimetry measurements in the anesthetized nonhuman primate with ExpG.

In addition, many of the monkeys used in the current study were originally part of a follow-up to the studies of Hare.^{9,10} Some of the current monkeys were fed memantine, an NMDA glutamate open-channel blocker that may rescue neurons through its blockade of excessive glutamate receptor activation,¹¹⁻¹³ for the duration of their ExpG. Early endpoints in ExpG were used, and correlations between elevated IOP exposure, axon loss, GDx VCC and electrophysiology parameters, and effects of memantine on those measures were also investigated.

MATERIALS AND METHODS

All animal studies were performed in accordance with institutional guidelines approved by the University of Wisconsin Research Animal Resources Center and in adherence to the ARVO Statement for the Use of Animals in Ophthalmic and Vision Research.

Cynomolgus monkeys (*Macaca fascicularis*) of either sex, weighing 2.3 to 6.9 kg were studied. ExpG was induced unilaterally in 25 monkeys by laser scarification of the trabecular meshwork,^{2,14} with a target IOP of 30 to 40 mmHg. IOP was monitored weekly under ketamine anesthesia by Goldmann applanation tonometry^{15,16} and occasionally with a Tonopen.¹⁷ GDx VCC scans, stereophotographs, and multifocal visual evoked potential (mfVEP) data were collected at

TABLE 1. GDx VCC Parameters Versus c/d Changes in ExpG

	Control Eyes N = 9	$\Delta c/d$		
		0–0.1 N = 9	0.15–0.2 N = 7	≥ 0.4 N = 4
TSNIT ellipse avg.	52.96 \pm 1.99	48.74 \pm 1.52	47.55 \pm 2.96	37.68 \pm 3.80
Avg. thickness	45.00 \pm 1.49	42.67 \pm 1.11	41.86 \pm 2.22	36.75 \pm 2.95
Superior avg.	64.56 \pm 2.99	61.28 \pm 2.57	56.63 \pm 4.54	40.37 \pm 2.47
Inferior avg.	59.11 \pm 2.74	55.48 \pm 2.09	51.94 \pm 3.82	39.57 \pm 5.79
SD	22.80 \pm 2.05	21.97 \pm 1.31	18.30 \pm 1.94	9.43 \pm 1.87
Change from baseline				
TSNIT ellipse avg.	0.10 \pm 0.31	–3.86 \pm 0.96*	–6.12 \pm 2.35*	–12.74 \pm 4.28
Avg. thickness	–0.05 \pm 0.28	–2.78 \pm 1.04*	–3.31 \pm 1.83	–6.92 \pm 4.12
Superior avg.	0.03 \pm 0.46	–5.30 \pm 1.89*	–9.57 \pm 3.02*	–18.67 \pm 4.61*
Inferior avg.	0.59 \pm 0.53	–4.01 \pm 1.39*	–9.06 \pm 3.22*	–19.72 \pm 5.51*
SD	0.19 \pm 0.46	–2.95 \pm 0.94*	–6.73 \pm 1.19*	–14.30 \pm 2.91*

Control eye values represent those taken in the Fellow eyes at the same time as when $\Delta c/d$ was 0.0 to 0.1 in ExpG eyes. Baseline scans are those taken prior to lasering and were used to calculate the changes in GDx parameters from baseline for the indicated amount of damage. c/d, cup-to-disc ratio; Avg., average.

Data are mean \pm SEM in micrometers.

* Significantly different from baseline by the two-tailed paired *t*-test; *P* < 0.05.

baseline and every 6 to 8 weeks until euthanasia. Not all monkeys received all tests.

Prior to lasering and after ExpG induction (1–11 months), 11 monkeys were started on a diet containing memantine (1-amino-3,5-dimethyladamantane; Allergan, Inc., Irvine, CA) in fruit, beginning at 2 mg/kg/day and ramping up over a 4-week period to 8 mg/kg/day). The remaining monkeys (no memantine) were either fed fruit or received no treatment. Plasma samples were collected at baseline and after 1 week at the 8 mg/kg dosage and every 6 to 8 weeks thereafter. These were analyzed at Allergan, Inc., using an internal standard method in combination with HPLC as described previously.⁹ A target plasma concentration of 1 μ M was desired prior to lasering.

When there was detectable loss of optic nerve head tissue in ExpG monkeys that did not receive memantine, as assessed by stereobiomicroscopic examination, monkeys were anesthetized with pentobarbital anesthesia and euthanized by exsanguination with PBS followed by perfusion through the heart with 2% to 4% paraformaldehyde. Optic nerves were prepared for axon counting and morphologic analysis.

GDx VCC

For establishing the techniques and to evaluate GDx parameters for use in monkeys, 12 monkeys with unilateral ExpG (eight from the group above and four additional female cynomolus [6–7 years old from an unrelated study]) and one rhesus monkey (female, 21 years with elevated IOP resulting from intraocular manipulations as part of another study) were used. Data from these last five monkeys were included only in Table 1. Parameters that were evaluated included the coefficient of variation of common measures, effects of lens opacity on the coefficient of variation, image quality with and without contact lenses measured on the same day, and correlation with cup-to-disc (c/d) ratio.

For GDx measurements, monkeys were anesthetized with a combination of intramuscular ketamine (10–15 mg/kg) and intramuscular medetomidine (30–60 μ g/kg), followed by inhalation isoflurane. Monkeys were maintained at, or near, surgical anesthetic depth for the scanning procedure. IOP (Goldmann applanation tonometer), corneal curvature (Reichert keratometer), and refraction (Hartinger-coincidence) were measured at each session. Axial length measurements (Sonomed A5500 A-Scan; Sonomed, Inc., Lake Success, NY) were taken at some time points. Slit-lamp biomicroscopic examinations were performed monthly. A 10-mm plano contact lens was applied to ensure adequate corneal hydration and clarity. Refraction and curvature

measurements were repeated after application of the lens, and values were entered into the patient focal correction field. A motorized head-holder with remote control was used to make fine adjustments in position to facilitate matching alignment to the baseline image. A GDx1 VCC prototype system (Laser Diagnostic Technology, San Diego, CA) was used to acquire nerve fiber layer (NFL) thickness measurements.¹⁸ Corneal compensation was calculated at baseline and verified by three or more compensated macular scans at each time point. A new compensation was calculated if retardance or corneal axis values were variable. During each session, three to five separate peripapillary scans were taken and a mean was created. The scan head was realigned between scans to generate discrete images. Variability (coefficient of variation) for the parameters was determined for Fellow normal eyes during intervals of 22 to 36 days, during which eyes were scanned three or four times. The GDx VCC system and parameters are described in greater detail elsewhere.^{19–21}

Stereoscopic color fundus photographs were taken on each scan day and used to evaluate the c/d ratio for each eye. If animals had both horizontal and vertical c/d ratio readings, the latter was used. In some eyes, an average of horizontal and vertical was used, for example, if one eye had horizontal and vertical evaluations and the other did not. IOP was lowered pharmacologically, starting the day before imaging, with Timoptic-XE (0.5% timolol maleate in gel-forming vehicle; Merck & Co., West Point, PA), and if necessary PGF2 α -isopropyl ester (2 μ g in 5 μ l saline; Cayman Chemical, Ann Arbor, MD), to reverse possible disc cupping because of compliance rather than tissue loss in ExpG eyes.

Electrophysiology

The mfVEPs were recorded with the methods presented in a recent publication.²² Root mean square (RMS) signal-to-noise ratio (SNR) determinations of the second-order (first slice) kernel (K2.1) mfVEP response (central 21° of the visual field) were compared in all statistical analyses. Linear regression analysis was applied to the scatter plots, and *P* values ≤ 0.05 were adopted as the level of significance. *t*-tests (two sample assuming unequal variances) were carried out on nonmemantine and memantine comparisons both at baseline and at study termination.

Axon Counts and Morphology

Optic nerves of 14 pairs of eyes with unilateral laser-induced ExpG were evaluated morphologically for optic nerve damage. Seven of the

animals had been treated with memantine, four were treated with vehicle, and three received no treatment. Because monkeys were in two different groups (each group containing memantine and no-memantine animals) as part of another study and were euthanized at different times, the optic nerve processing varied as conditions were optimized for tissue collection for the parent study. For six monkeys (two memantine, four no-memantine), following exsanguination with PBS and perfusion through the heart with 2% paraformaldehyde/0.1M phosphate buffer (PB), pH 7.4, the eyes with optic nerves attached were enucleated and placed in 2% paraformaldehyde/0.1M PB for 3 hours then transferred to 30% sucrose and stored for the parent study. Subsequently, after several months, the optic nerves were transferred to Ito's fixative.²³ For the other eight monkeys (five memantine, three no-memantine), following exsanguination with PBS, the eyes were enucleated, and the optic nerves were dissected 1 to 2 mm behind the globe and placed in Ito's fixative. All of the optic nerves were embedded in Epon and then semithin cross-sectioned with an Ultracut E (Reichert Jung, Vienna, Austria) and subsequently stained with toluidine blue. Sections were viewed with an Aristoplan microscope (Ernst Leitz, Wetzlar, Germany) and photographed with a Leica DC 500 camera (Leica Camera AG, Solms, Germany). Despite the differences in fixation types, the axon quantification was possible except in three Fellow eyes in which the center of the nerve was not preserved well enough for quantification.

Determination of Optic Nerve Changes

Axon counts were determined in accordance to our previous reports²⁴⁻²⁷ based on the method of Quigley.¹ Briefly, the area of the entire nerve, excluding the meninges, was measured. The area containing the nerve fiber bundles and the area of connective tissue between the nerve fiber bundles and surrounding the central retinal vessels were measured separately. For determination of the axon number, the cross-section of the optic nerve was divided into eight sectors. In each sector, axons in five sample areas of 1000 μm^2 were counted. These sample areas extended from the central to the peripheral nerve at equal distances from each other. The mean of all measurements was multiplied by the nerve fiber area to yield the total axon counts (see Table 4).

Data Analysis

Linear regression analysis was used to compare correlations between two parameters.

Area under the Curve. Once IOP in the ExpG eyes was ≥ 25 mmHg and the difference ExpG-Fellow IOP was ≥ 5 mmHg initially, then the difference at each time point was plotted versus time. The area under this difference curve was integrated using Sigma Plot v8.0 (Systat Software, Inc., San Jose, CA).

Paired and Unpaired t-tests. Two-tailed paired and unpaired *t*-tests compare differences to 0.0 or ratios to 1.0. Significance was designated at $P < 0.05$.

RESULTS

IOP and Cumulative IOP Insult

IOP (mean \pm SEM) in ExpG eyes from the time of initial elevation of ≥ 25 mmHg until euthanasia averaged 30.45 ± 1.74 mmHg while Fellow control eyes averaged 16.52 ± 0.36 mmHg ($n = 27$). In no-memantine ExpG eyes, IOP during the same interval was 32.29 ± 2.54 mmHg. In memantine ExpG eyes, the corresponding IOP was 28.11 ± 2.23 mmHg. Cumulative IOP Insult (CII, mmHg \times days) analysis for ExpG and Fellow control eyes showed that for all monkeys in the study, there was a tendency toward but no significant difference in IOP elevation exposure comparing memantine-

treated and no-memantine-treated monkeys (CII memantine = 1276 ± 240 ; CII no-memantine = 1804 ± 283 , $P = 0.183$, unpaired *t*-test). Also, the average IOP difference between ExpG and Fellow eyes calculated by CII/days was no different comparing memantine-treated and no-memantine-treated monkeys (mean mmHg difference, memantine = 12.6 ± 2.1 ; no-memantine = 15.5 ± 2.3 , $P = 0.36$, unpaired *t*-test).

Serum memantine ranged from 0.4 to 3.9 μM over the duration of the study.

GDx VCC

Figure 1 is an example of a GDx VCC scan in monkey K560 with ExpG in the right eye demonstrating severe nerve fiber layer thinning. Table 1 shows a progressive decrease in commonly examined GDx VCC parameter values relative to baseline as the c/d ratio increased in ExpG eyes. Mean intercession coefficients of variation for these parameters measured three to four times in four Fellow eyes without lens opacities during a 22- to 36-day interval ranged from 3.5% to 5.5%. Lens opacities slightly increased the coefficient of variation (clear lens vs. opacity: average thickness, 3.5% vs. 4.2%; TSNIT SD, 5.0% vs. 11.8%; inferior average, 5.5% vs. 7.3%). Image-quality scores, which reflect overall image quality, image intensity, image vignetting, illumination, and contrast, were greatly improved when a contact lens was used (e.g., 4/35 failures [scores less than 70 out of 100] with a contact lens vs. 16/35 failures in the same seven eyes without a contact lens). Significant changes were detected comparing baseline and terminal refractions (diopters \pm SEM) in ExpG eyes (baseline, -1.11 ± 0.26 ; terminal -2.67 ± 0.47 , $P = 0.002$, $n = 9$).

There was strong positive correlation between the percentage change ($100\% \times [\text{ExpG} - \text{Cont}]/\text{Cont}$) in GDx parameters from scans taken just prior to euthanasia compared with the axon loss ratio (Figs. 2A, 2B, Table 2). Strong correlations were also found with the percentage change in GDx parameters in the ExpG eyes and the actual axon counts (Figs. 2C, 2D) as well as with the actual GDx parameter values for all eyes and the actual axon counts (Figs. 2E, 2F).

Nerve fiber layer thickness was significantly decreased in ExpG compared with Fellow eyes in both memantine and no-memantine groups (Table 3). There were no significant differences in GDx VCC parameters comparing ExpG eyes from memantine-treated and no-memantine-treated monkeys by the unpaired *t*-test. Data are from terminal scans closest to the date of euthanasia.

Optic Nerve Changes and Axon Counts

There were marked differences between animals in the amount of optic nerve damage in the ExpG eyes. The percent change in axon counts in ExpG versus Fellow eyes was correlated with the mean change in IOP exposure with two exceptions in the memantine group. The mean change in IOP was calculated from the CII/duration of IOP elevation from the time IOP was 5 mmHg or more different from the Fellow eye until euthanasia.

The axon counts in ExpG eyes varied from 400,000 to 500,000 (three eyes), 500,000 to 700,000 (five eyes), and 700,000 to 1,000,000 (six eyes). The distribution of axon damage showed regional differences within the nerve fiber cross-sections. In most nerves with axon counts of 700,000 to 1,000,000, there was a nearly polar orientation of the damaged areas, which were only seen in the periphery of opposing parts of the circumference (Fig. 3A). The morphology of the damaged areas was different in the two regions. In the less damaged areas (blue areas in the schematic drawing), the nerve fiber bundles were still clearly separated from each other by

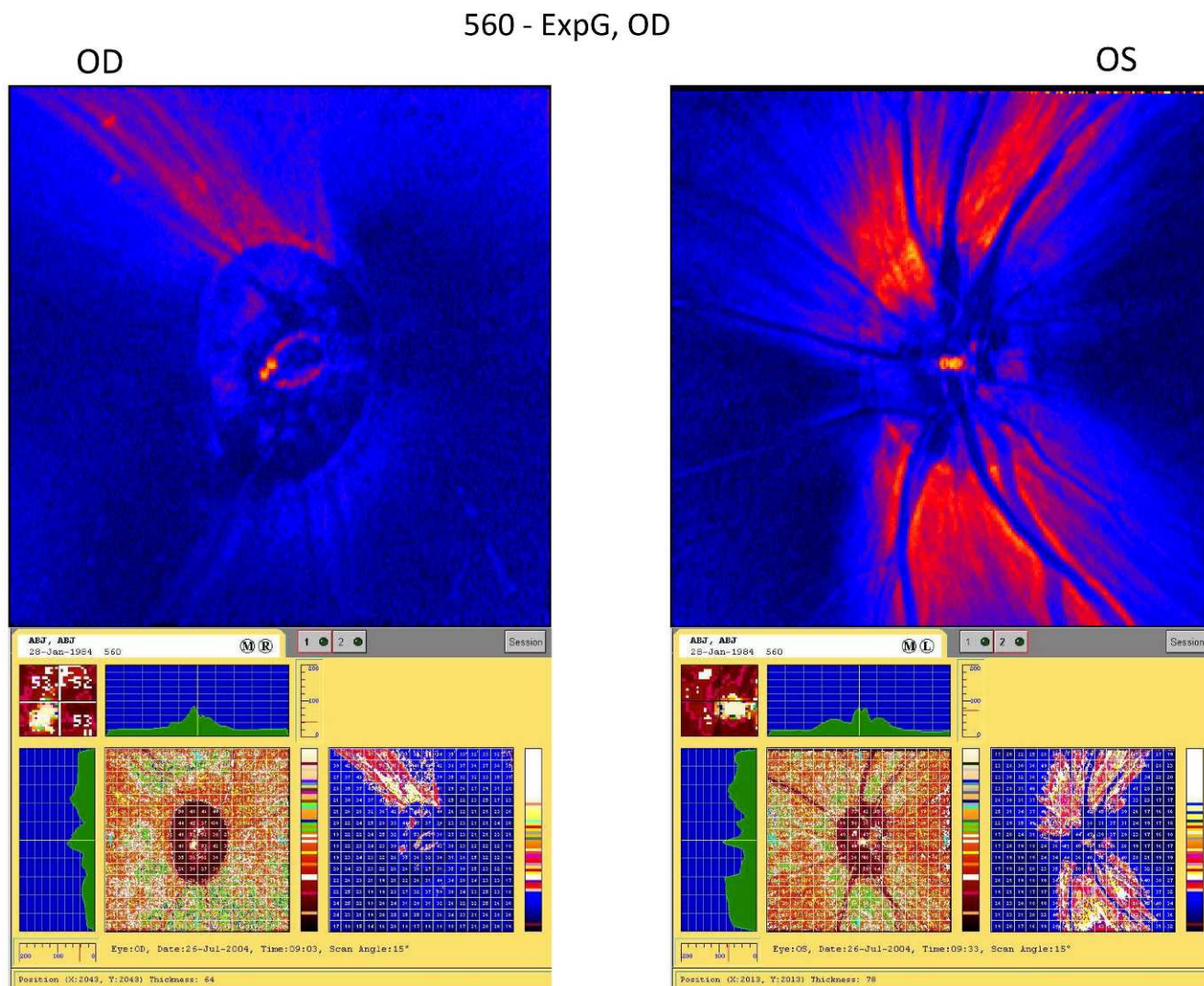


FIGURE 1. Example of a GDx VCC scan from a monkey with ExpG. The GDx scan for monkey K560 shows severe thinning of the nerve fiber layers in the superior and inferior quadrants of the glaucomatous right eye (see also Table 2 for terminal GDx VCC values).

connective tissue septae, which were slightly thickened compared with the normal control eye and showed a thickened sheath of astroglial cells (Fig. 3D). Within the bundles, the size of the astroglial cells appeared increased and there were spherical inclusions of myelin figures (Fig. 3D).

In areas marked as red in the schematic drawing, parts of the connective tissue septae appeared destroyed and displaced by numerous cells, most of them with large nuclei and some with dark inclusions. In between the cells, remnants of myelin and single myelinated axons were present (Fig. 3E). Most parts of the nerve, however, still appeared unchanged (white areas in Fig. 3A, corresponding to 3F).

With increasing loss of axons, the morphology of areas drawn blue and red in the schematic drawings were larger. In most eyes with axon counts of 500,000 to 700,000, there were still pronounced regional differences. In three of the five eyes, the center of the nerve was still unchanged. However, nearly the entire periphery showed the severe changes (red, Fig. 3B). This was also true for the other two eyes, but in these eyes slight changes were present throughout the entire cross-section of the nerve. In the three eyes with only 400,000 to 500,000 remaining axons, the entire nerve was damaged but more apparent in the periphery than the center of the nerve (Fig. 3C).

Axon counts in ExpG eyes both from monkeys that did not receive memantine and from those that did receive memantine were significantly decreased relative to Fellow eyes. There was no significant difference in axon loss comparing ExpG with Fellow eyes from no-memantine- and memantine-treated monkeys (unpaired *t*-test, $P = 0.54$) (Table 4). Of the seven eyes treated with memantine, two had axon counts of 400,000 to 500,000, one had counts of 600,000, and four had axon counts between 800,000 and 1,000,000. There were no differences in patterns of axon loss, areas with axon damage, and morphology of these areas in ExpG optic nerves from monkeys that did not receive memantine compared with those that did receive memantine. In all ExpG optic nerves (memantine and no-memantine), the center of the nerve remained unchanged in the less affected eyes, and the periphery was more damaged than the central area.

The percentage of the optic nerve area composed of connective tissue septa was significantly greater in ExpG than in Fellow eyes from all monkeys examined. There was no difference in the percentage of the optic nerve containing connective tissue septa in ExpG as a result of memantine in the diet. Total optic nerve area was no different in ExpG compared with Fellow eyes.

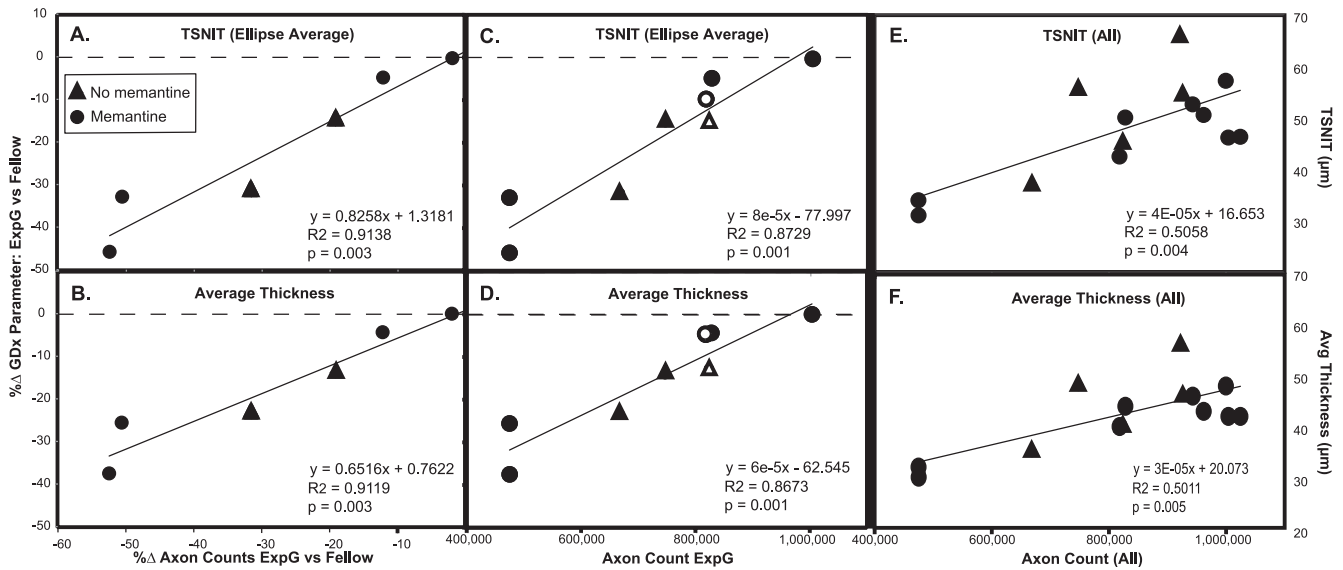


FIGURE 2. TSNIT or average thickness changes in ExpG compared with Fellow eyes as a function of axon counts. Common GDX measures were highly correlated with percent change (%Δ) in axon counts in ExpG versus Fellow eyes (A, B) and with actual axon counts in ExpG eyes (C, D). The absolute value of GDX measures considering all eyes was also correlated with axon counts (E, F). Similar correlations were found with other GDX measures (superior average and inferior average). More axon count values were available for ExpG eyes than for Fellow eyes (open symbols indicate ExpG eyes where there were no corresponding Fellow eye axon counts, also see Table 4).

Electrophysiology

At baseline, there were no significant differences between the eyes (ExpG or Fellow) in RMS amplitude SNR for either the no-memantine or memantine groups (Table 5). Baseline values for the memantine group were lower (but not significantly) than for the no-memantine group. As expected, in animals that did not receive memantine, the ExpG eyes exhibited significantly lower final RMS amplitude SNR compared with baseline determinations ($P = 0.004$) and compared with Fellow eyes ($P = 0.007$). Note also that none of the two-sample *t*-test statistical comparisons for the memantine group were statistically significant (Baseline ExpG vs. Baseline Fellow; Final ExpG vs. Final Fellow; Baseline ExpG vs. Final ExpG; Baseline Fellow vs. Final Fellow). Final mean amplitudes for memantine ExpG eyes were higher (but not significantly) than were those for no-memantine ExpG eyes. Final amplitudes for Fellow eyes remained lower in the memantine group compared with the no-memantine group, as they did at baseline.

DISCUSSION

In conducting GDX VCC measurements in nonhuman primates, there are several potential sources of variability that should be monitored. Subjects cannot fixate, so the operator has greater responsibility for alignment. Vigilance is required to align images consistently from one session to the next, as with human patients who do not fixate well or vary in the ability to comfortably position their head and neck from visit to visit. Contact lenses, which increase image quality and are useful to maintain corneal hydration, can change refraction, apparent corneal curvature, and axial length values. There was a tendency in the current study for monkeys to become myopic over time in the ExpG eye. Refraction values cannot be assumed to be constant. This change might impact the computation of some values made by the software. Collecting session-specific information will help assess the impact of this potential source of variability. Collecting multiple discrete scans at each time point, especially at baseline, to get a measure of individual eye variability, can reduce confidence

TABLE 2. Terminal GDX VCC Values for Axon Comparisons in Figure 2

Monkey No.	GDX VCC Parameter (μm)							
	TSNIT (Ellipse Average)		Average Thickness		Superior Average		Inferior Average	
	ExpG	Cont	ExpG	Cont	ExpG	Cont	ExpG	Cont
K568	56.38	66.46	49.00	57.00	62.34	81.62	70.83	79.18
K639	37.67	55.23	36.00	47.00	44.67	63.73	41.20	61.11
K640	45.84	54.27	41.00	47.00	56.32	72.44	50.55	61.11
K560	31.02	53.38	30.00	46.00	42.10	62.30	25.94	60.89
K564	33.96	50.57	32.00	43.00	38.92	65.54	31.07	52.87
K576	42.48	47.06	40.00	42.00	39.34	39.21	51.31	53.41
K630	46.17	46.32	42.00	42.00	58.28	55.13	49.48	53.97
K645	50.07	52.63	44.00	46.00	68.48*	54.38	51.28	60.24

* Value not included in regression analysis; corneal scar increased variability of value in this quadrant.

TABLE 3. Terminal GDx VCC Parameters: No-Memantine Versus Memantine

	ExpG	Fellow	ExpG BL	Fellow BL
No memantine (<i>n</i> = 7)				
TSNIT	44.11 ± 3.77†‡	55.20 ± 2.08*	50.69 ± 1.20	51.74 ± 1.61
Avg. thickness	39.00 ± 2.81†‡	47.29 ± 1.90*	43.14 ± 1.24	44.14 ± 1.61
Superior avg.	52.62 ± 4.41*†‡	67.99 ± 2.74*	62.32 ± 1.51	63.65 ± 1.57
Inferior avg.	50.08 ± 5.33	61.38 ± 3.16	57.30 ± 1.74	59.20 ± 2.75
Memantine (<i>n</i> = 8)				
TSNIT	41.45 ± 2.58†	50.28 ± 1.47	49.77 ± 1.49	51.03 ± 1.46
Avg. thickness	37.25 ± 1.84†	43.38 ± 1.12	42.25 ± 1.15	44.08 ± 1.43
Superior avg.	50.69 ± 4.28	58.79 ± 3.44	62.77 ± 2.62	62.25 ± 1.87
Inferior avg.	43.74 ± 4.13*†	57.36 ± 2.26	57.10 ± 1.75	56.46 ± 1.64

ExpG eyes from no-memantine- and memantine-treated monkeys had similar elevated IOP exposure at the time of the final scans. Cumulative IOP Insult (CII, Δ mmHg \times days) of IOP difference versus time (see Methods). No-memantine = 1213 \pm 216; memantine = 937 \pm 247; *P* = 0.423, unpaired *t*-test. Fellow, contralateral eye without ExpG; BL, baseline.

GDx VCC parameters are mean \pm SEM in micrometers.

* Paired *t*-test significantly different from BL.

† Paired *t*-test significantly different from the Fellow eye.

‡ Paired *t*-test significantly different from the Fellow eye after correction for BL.

intervals, increasing the likelihood of identifying meaningful change. Inter- and intrasession variability reported in the current study were similar to those obtained in an unrelated study of eyes of 10 normal cynomolgus monkeys (unreported data).

Terminal GDx parameters, especially TSNIT, were highly correlated with axon counts and c/d ratio changes. The correlation of individual eye GDx parameter values with the corresponding axon counts, although significant, was not as strong as when the GDx results were first expressed as a

percentage change in ExpG compared with Fellow eyes (Fig. 2). This suggests that there are individual animal traits that can cause variation in the GDx measures or in the axon counts. Unlike the Hare study,¹⁰ the current study did not detect any memantine-related effects on structural parameters during ExpG. However, only monkeys with the highest mean IOPs were studied by Hare, and the structural measures were done with the Heidelberg Retina Tomograph. The current study also did not detect any significant decrease in optic nerve area, presumably because of the relatively mild loss of axons (<35%

TABLE 4. Axon Counts: No-Memantine Versus Memantine

Monkey No.	Axon Count		Total Optic Nerve Area (mm ²)		Septa Including Glia (% Optic Nerve Area)		Connective Tissue Septa (% Optic Nerve Area)	
	ExpG	Fellow	ExpG	Fellow	ExpG	Fellow	ExpG	Fellow
No memantine								
K545	622,640	975,188	4.00	5.71	14.0	n.a.	1.64	1.75
K547	614,813	942,941	4.74	4.94	15.5	10.7	5.22	2.34
K640	823,680	n.a.	7.20	n.a.	10.0	n.a.	3.29	1.67
K568	746,941	922,756	4.38	4.27	8.7	9.4	1.96	2.00
K570	401,857	957,187	5.04	5.65	15.2	7.5	2.65	2.75
K581	563,581	1,053,519	3.97	5.43	16.0	n.a.	2.06	2.55
K639	667,722†	925,936	5.74	5.02	11.2	n.a.	2.83	2.50
Mean	634,462*	962,921	5.01	5.17	12.94	9.20	2.81	2.22
SEM	50,994	19,809	0.43	0.22	1.11	0.93	0.46	0.16
Memantine								
K544	612,797	964,429	3.93	4.91	11.0	6.7	4.11	1.91
K549	802,935	n.a.	5.23	4.81	11.0	n.a.	3.61	3.26
K560	475,151	999,648	6.30	6.18	9.3	12.0	2.76	2.98
K564	474,918†	961,779	4.07	4.22	10.3	7.3	1.13	1.07
K576	818,209	n.a.	6.51	6.09	14.5	n.a.	3.92	n.a.
K645	828,028†	943,033	5.11	5.90	25.6	16.2	5.60	4.33
K630	1,003,953	1,024,456	4.31	4.14	10.0	8.0	2.89	1.62
Mean	716,570*	990,179	5.07	5.18	13.10	10.04	3.43	2.53
SEM	70,022	16,602	0.39	0.33	2.18	1.80	0.52	0.49
Mean all	675,516*	976,550	5.04	5.17	13.02*	9.73	3.12*	2.36
SEM	45,275	12,989	0.28	0.20	1.17	1.13	0.34	0.24

* Significantly different from contralateral fellow eye where values from both eyes were available (two-tailed paired *t*-test for differences compared to 0.0); n.a., not available.

† Axon diagram shown in Figure 3.

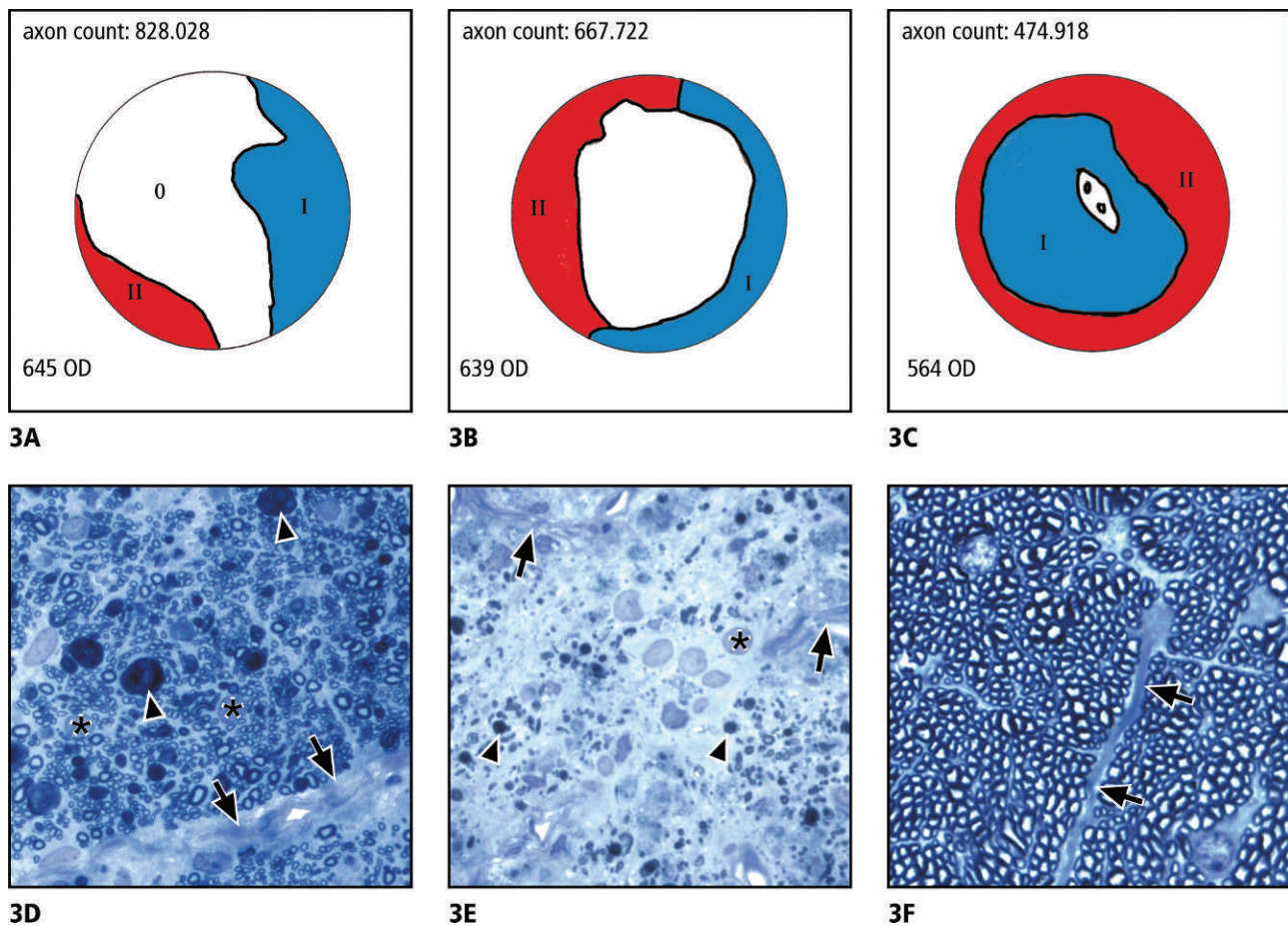


FIGURE 3. Morphology of optic nerve damage as a result of ExpG. (A–C) Schematic drawings showing typical distributions of severely damaged (red), slightly damaged (blue), and histologically unchanged (white) areas in eyes with axon counts of (A) approximately 800,000; (B) approximately 500,000 to 600,000; and (C) approximately 400,000–500,000. (D–F) Semithin cross-sections of optic nerves (Richardson's stain). (D) Micrograph of a less damaged area (blue areas in the schematic drawings A–C). The nerve fiber bundles are still separated from each other by connective tissue septae (arrows), which, at places, are thickened and show a thickened sheath of glial cells (asterisks). Singular axons are destroyed and appear as spherical inclusions of myelin figures (arrowheads). (E) Micrograph of a severely damaged area (red areas in the schematic drawings A–C). Parts of the connective tissue septae appear destroyed (arrows) and displaced by numerous cells with large nuclei (asterisk). In the region of the previous bundles, remnants of myelin (arrowheads) are present. (F) Normal unaffected region of a nerve with the nerve fiber bundles separated from each other by connective tissue septae (arrows).

loss comparing ExpG to Fellow axon counts) and shorter duration of IOP elevation as compared with other studies.^{1,28}

Evidence for a neuroprotective effect of memantine on ganglion cell function in this study could manifest as either enhanced or stabilized mfVEP from ExpG eyes. The authors found that mfVEP from the central stimulus element was sensitive to ExpG: Animals receiving no memantine exhibited significantly lower mfVEP amplitudes in ExpG eyes compared with baseline in the same eye or the final value in the Fellow eye. In contrast, ExpG eyes from memantine-treated animals had higher overall mean amplitudes that were not significantly different relative to baseline in the same eye and final test in the Fellow eye (Table 5). Note that at baseline the mfVEP RMS SNR determinations of the ExpG and Fellow eyes (5.94 ± 0.91 and 6.58 ± 1.00) of the group of animals that were administered memantine tended to be lower (but not significantly) than for the ExpG and Fellow eyes (7.04 ± 0.85 and 7.17 ± 1.23) of the group of animals that did not receive memantine. In addition to inherent variability in mfVEP recordings, memantine plasma levels at the time of sacrifice also were quite variable. Serum levels of memantine were not maintained at the $1 \mu\text{M}$ level achieved in the Hare studies although early on in their study, levels fluctuated as well.⁹

Given baseline differences, serum memantine levels, and the variability between animals and test sessions in this study, intra-ocular comparisons rather than between-group comparisons are best suited for evaluating the effects of memantine. As noted, there was a significant interocular difference between the mfVEP of ExpG and Fellow eyes of the no-memantine group; however, there was no statistical difference between ExpG and Fellow eyes in memantine-treated animals. The absence of a difference in mfVEP between ExpG and Fellow eyes in the memantine group is therefore consistent with a stabilization of mfVEP of the ExpG eyes, and thus also consistent with, but not probative of, a possible neuroprotective role of memantine on retinal ganglion cells.

There are several possible reasons why the functional (mfVEP) and structural measures (GDx and axon counts) were not always correlated. Animals with electrophysiologic testing were a smaller subset of the animals with both GDx and axon counts. There are also differences in the variance of the functional and structural measures. The coefficient of variation (SD/mean) for mfVEP RMS SNR is approximately double that of GDx and axon counts. In addition, the relationship between functional and structural measures is not likely to be linear across cell layers or uniform within all animals. Most

TABLE 5. Multifocal VEP K2.1 RMS SNR in ExpG and Fellow Eyes: Baseline and Terminal

Monkey No.	Baseline RMS SNR		Final RMS SNR	
	ExpG	Fellow	ExpG	Fellow
No memantine				
K543	5.906	4.522	4.350	3.204
K547	10.899	11.819	4.700	10.863
K568	6.355	5.491	4.795	4.039
K570	9.172	10.966	1.614	12.095
K574	5.920	5.333	3.378	9.475
K639	3.885	10.315	1.752‡	7.638
K640	5.839	3.831	3.599	9.804
K625	8.379	5.081	5.052	6.465
Mean ± SEM	7.04 ± 0.85	7.17 ± 1.23	3.66 ± 0.51*†	7.95 ± 1.21
Memantine				
K541	8.564	7.640	3.586	4.936
K544	7.665	5.106	2.685	11.751
K549	7.575	6.692	1.617	2.920
K560	5.009	6.064	8.554	8.105
K564	11.061	6.839	7.618‡	3.586
K576	5.162	4.172	5.497	11.029
K630	3.802	11.533	4.470	6.237
K645	4.614	4.472	4.575‡	2.062
K595	1.968	11.245	3.180	5.368
K608	3.944	2.035	1.708	2.613
Mean ± SEM	5.94 ± 0.91	6.58 ± 1.00	4.35 ± 0.78	5.86 ± 1.15

t-test: two sample assuming unequal variances.

* Significantly different from baseline, $P = 0.004$.

† Significantly different from the final Fellow eye value, $P = 0.007$.

‡ Axon diagram shown in Figure 3.

importantly, the mfVEP measure is derived from the macular stimulus whereas the most severe axonal damage was located in the peripheral optic nerve (Fig. 3).

Despite these limitations, the authors' mfVEP results are similar to the VEP findings of Hare⁹ in that they suggest that memantine may be providing some neuroprotection of the retinal ganglion cells or other cellular structures subserving the central cortical response. In the Hare studies,⁹ functional measures demonstrated that memantine treatment delayed but did not prevent the amplitude reduction in the multifocal electroretinogram and visually evoked cortical potential. Amplitude differences were most noticeable at 3 to 5 months after IOP elevation. For monkeys with moderate IOP elevation, memantine treatment was associated with enhanced survival of retinal ganglion cells, especially in the inferior retina. However, they were uncertain if memantine was enhancing the electrophysiology response versus protecting retinal ganglion cells and their axons. It is possible that memantine treatment enhances the ability of surviving retinal ganglion cells to drive activity in the visual cortex, that is, memantine treatment may be associated with plastic changes occurring at more central levels of the visual pathway. Indeed, there was significantly less neuron shrinkage in the lateral geniculate nucleus (LGN) of the memantine-treated than in the vehicle-treated control group even though there was no difference in optic nerve fiber loss.²⁹ LGN neurons showed reduced dendrite complexity and length that were modified by NMDA receptor blockade with memantine.³⁰

As shown by Harwerth,⁴ electrophysiologic methods can be as sensitive as standard automated perimetry (SAP) in assessing neural loss from ExpG in nonhuman primates. Visual sensitivity losses were not correlated with retinal ganglion cell losses until a substantial number of neurons were lost. There is a period of progressive neural loss that cannot be detected by SAP as is the

case with human glaucoma.³¹ However, objective measures such as the photopic negative response, which represents the linear sum of signals from all of the retinal ganglion cells, might detect a proportional decrease in neuronal loss.⁴

At any given point of glaucoma progression, it is speculated that the total retinal ganglion cell population includes a mixed population of normal, dysfunctional, nonviable, and atrophic retinal ganglion cells in various stages of degeneration. Current clinical imaging technologies are capable only of quantifying structural changes in retinal ganglion cell axons but do not specify the level of retinal ganglion cell dysfunction.³²

Several imaging technologies are now available that are useful for detecting progression during early stages of the glaucoma before functional changes can be detected.^{7,33-35} Our studies confirm that GDx VCC can be used in monkey ExpG studies to detect early retinal structural changes that may or may not lead to central functional changes. Although the authors' studies show a strong correlation between GDx VCC parameters and axon loss in ExpG, this correlation may not always hold if acute axonal injury affecting birefringence precedes structural loss. Fortune et al. found that a decline in GDx parameters preceded retinal nerve fiber layer (RNFL) thickness changes in monkeys after optic nerve transection³⁶ and after intravitreal colchicine injection.³⁷ Thus, measures of birefringence may provide data on RNFL disease that are complementary to other imaging modalities.

References

1. Quigley HA, Addicks EM, Green WR. Optic nerve damage in human glaucoma. III. Quantitative correlation of nerve fiber loss and visual field defect in glaucoma, ischemic neuropathy, papilledema, and toxic neuropathy. *Arch Ophthalmol*. 1982; 100:135-146.

2. Gaasterland D, Kupfer C. Experimental glaucoma in the rhesus monkey. *Invest Ophthalmol*. 1974;13:455-457.
3. Gabelt BT, Ver Hoeve JN, Kaufman PL. Intraocular pressure elevation: laser photocoagulation of the trabecular meshwork. In: LA, Levin, Di Polo A, eds. *Ocular Neuroprotection*. New York: New York, Marcel Dekker; 2003:47-84.
4. Harwerth RS, Crawford ML, Frishman LJ, Viswanathan S, Smith EL III, Carter-Dawson L. Visual field defects and neural losses from experimental glaucoma. *Prog Retinal Eye Res*. 2002;21:91-125.
5. Tuulonen A, Alraksinen PJ. Initial glaucomatous optic disk and retinal nerve fiber layer abnormalities and their progression. *Am J Ophthalmol*. 1991;111:485-490.
6. Townsend KA, Wollstein G, Schuman JS. Imaging of the retinal nerve fibre layer for glaucoma. *Br J Ophthalmol*. 2009;93:139-143.
7. Medeiros FA, Alencar LM, Zangwill LM, et al. Detection of progressive retinal nerve fiber layer loss in glaucoma using scanning laser polarimetry with variable corneal compensation. *Invest Ophthalmol Vis Sci*. 2009;50:1675-1681.
8. Reus NJ, Lemij HG. Scanning laser polarimetry of the retinal nerve fiber layer in perimetrically unaffected eyes of glaucoma patients. *Ophthalmology*. 2004;111:2199-2203.
9. Hare WA, WoldeMussie E, Lai RK, et al. Efficacy and safety of memantine treatment for reduction of changes associated with experimental glaucoma in monkey, I: functional measures. *Invest Ophthalmol Vis Sci*. 2004;45:2625-2639.
10. Hare WA, WoldeMussie E, Weinreb RN, et al. Efficacy and safety of memantine treatment for reduction of changes associated with experimental glaucoma in monkey, II: structural measures. *Invest Ophthalmol Vis Sci*. 2004;45:2640-2651.
11. Osborne NN, Quack G. Memantine stimulates inositol phosphates production in neurones and nullifies n-methyl-D-aspartate-induced destruction of retinal neurones. *Neurochem Int*. 1992;21:329-336.
12. Lipton SA, Stamler JS. Actions of redox-related congeners of nitric oxide at the nmda receptor. *Neuropharmacology*. 1994;33:1229-1233.
13. Sucher NJ, Lipton SA, Dreyer EB. Molecular basis of glutamate toxicity in retinal ganglion cells. *Vis Res*. 1997;37:3483-3493.
14. Wamsley S, Gabelt BT, Dahl DB, et al. Vitreous glutamate concentration and axon loss in monkeys with experimental glaucoma. *Arch Ophthalmol*. 2005;123:64-70.
15. Kaufman PL, Davis GE. Minified Goldmann applanating prism for tonometry in monkeys and humans. *Arch Ophthalmol*. 1980;98:542-546.
16. Croft MA, Kiland J, Gange SJ, Aref A, Pelzek CD, Kaufman PL. Comparison of Goldmann tonometry measurements using creamer vs fluorescein in cynomolgus monkeys. In: Lakshminarayanan V, ed. *Basic and Clinical Applications of Vision Science. The Professore Jay M. Enoch Festschrift Volume, Documenta Ophthalmologica Proceedings Series, Vol. 60*. Dordrecht, Netherlands: Kluwer; 1997:213-216.
17. Peterson JA, Kiland JA, Croft MA, Kaufman PL. Intraocular pressure measurement in cynomolgus monkeys: Tono-pen versus manometry. *Invest Ophthalmol Vis Sci*. 1996;37:1197-1199.
18. Weinreb RN, Bowd C, Zangwill LM. Scanning laser polarimetry in monkey eyes using variable corneal polarization compensation. *J Glaucoma*. 2002;11:378-384.
19. Weinreb RN, Bowd C, Zangwill LM. Glaucoma detection using scanning laser polarimetry with variable corneal polarization compensation. *Arch Ophthalmol*. 2002;120:218-224.
20. Colen TP, Tang NEML, Mulder PGH, Lemij HG. Sensitivity and specificity of new GDx parameters. *J Glauc*. 2004;13:28-33.
21. Bagga H, Greenfield DS, Knighton RW. Scanning laser polarimetry with variable corneal compensation: identification and correction for corneal birefringence in eyes with macular disease. *Invest Ophthalmol Vis Sci*. 2003;44:1969-1976.
22. Maertz NA, Kim CBY, Nork TM, Lucarelli MJ, Kaufman PL, Ver Hoeve JN. Multifocal visual evoked potentials in the anesthetized non-human primate. *Curr Eye Res*. 2006;31:885-893.
23. Ito S, Karnovsky MJ. Formaldehyde-glutaraldehyde fixatives containing trinitro compounds. *J Cell Biol*. 1968;39:168a-169a.
24. Gottanka J, Flügel-Koch C, Martus P, Johnson DH. Correlation of pseudoexfoliative material and optic nerve damage in pseudoexfoliation syndrome. *Invest Ophthalmol Vis Sci*. 1997;38:2435-2446.
25. Gottanka J, Johnson DH, Martus P, Lütjen-Drecoll E. Severity of optic nerve damage in eyes with POAG is correlated with changes in the trabecular meshwork. *J Glauc*. 1997;6:123-132.
26. Gottanka J, Kirch W, Tamm ER. The origin of extrinsic nitrergic axons supplying the human eye. *J Anat*. 2005;206:225-229.
27. Tektas OY, Lütjen-Drecoll E, Scholz M. Qualitative and quantitative morphologic changes in the vasculature and extracellular matrix of the prelaminar optic nerve head in eyes with POAG. *Invest Ophthalmol Vis Sci*. 2010;51:5083-5091.
28. Yücel YH, Kaichman MW, Mizisin AP, Powell HC, Weinreb RN. Histomorphometric analysis of optic nerve changes in experimental glaucoma. *J Glaucoma*. 1999;8:38-45.
29. Yücel YH, Gupta N, Zhang Q, Mizisin AP, Kalichman MW, Weinreb RN. Memantine protects neurons from shrinkage in the lateral geniculate nucleus in experimental glaucoma. *Arch Ophthalmol*. 2006;124:217-225.
30. Ly T, Gupta N, Weinreb RN, Kaufman PL, Yücel YH. Dendrite plasticity in the lateral geniculate nucleus in primate glaucoma. *Vision Res*. 2011;51:243-250.
31. Quigley HA, Dunkelberger GR, Green WR. Chronic human glaucoma causing selectively greater loss of large optic nerve fibers. *Ophthalmology*. 1988;95:357-363.
32. Sehi M, Pinzon-Plazas M, Feuer WJ, Greenfield DS. Relationship between pattern electroretinogram, standard automated perimetry, and optic nerve structural assessments. *J Glauc*. 2009;18:608-617.
33. Kass MA, Heuer DK, Higginbotham EJ, et al. A randomized trial determines that topical ocular hypotensive medication delays or prevents the onset of primary open-angle glaucoma. *Arch Ophthalmol*. 2002;120:701-713.
34. Miglior S, Zeyen T, Pfeiffer N, et al. Results of the European glaucoma prevention study. *Ophthalmology*. 2005;112:366-375.
35. Reus NJ, Lemij HG. Relationships between standard automated perimetry, HRT confocal scanning laser ophthalmoscopy, and GDx VCC scanning laser polarimetry. *Invest Ophthalmol Vis Sci*. 2005;46:4182-4188.
36. Fortune B, Cull GA, Burgoyne CF. Relative course of retinal nerve fiber layer birefringence and thickness and retinal function changes after optic nerve transection. *Invest Ophthalmol Vis Sci*. 2008;49:4444-4452.
37. Fortune B, Wang L, Cull G, Cioffi GA. Intravitreal colchicine causes decreased rNFL birefringence without altering rNFL thickness. *Invest Ophthalmol Vis Sci*. 2008;49:255-261.